

# Hybrid Heuristic-aided Multi-scale Deep Learning Model for Maximizing the Received Signal Strength in Visible Light Communication

Suganya Pandarinathan<sup>1</sup>, R. K. Jeyachitra<sup>2</sup>

<sup>1,2</sup> Department of Electronics and Communication Engineering, National Institute of Technology  
Tiruchirappalli, Tamil Nadu, India- 620015.

<sup>1</sup>sugu0805@gmail.com, <sup>2</sup>jeyachitra@nitt.edu

**Corresponding author:** sugu0805@gmail.com

Article Received: 20 Feb 2025, Revised: 21 April 2025, Accepted: 03 May 2025

**Abstract-** LED-based Visible Light Communication (VLC) technology has excellent positional accuracy; according to some articles, it can reach centimetre-level accuracy. VLC is unique because it uses a lot of unlicensed bandwidth and is naturally energy-efficient. Notably, VLC proves suitable in environments like hospitals, aircraft and mining zones, where concerns about electromagnetic contamination arise. As a result, indoor localization has identified a promising alternative: Indoor Visible Light Positioning (VLP), which is a hinging on VLC techniques. The implications extend to its potential integration in safety and monitoring systems within nuclear mining operations, where robust, non-RF communication is beneficial. It's important to note that theoretical evaluations of the accuracy of indoor VLC positioning systems based on the Received Signal Strength Indicator (RSSI) algorithm are still lacking. Some research projects have looked into integrating deep learning to improve translation procedures. A deep learning approach is proposed for VLC networks to accomplish effective performance. The main aim of this system is to maximize the RSS in the network. Firstly, the data attributes regarding the signal are collected and fed into the model of a Multiscale One-Dimensional Convolutional Neural Network with Symmetric Convolution (M1D-CNN-SC), in which the hyperparameters are optimally selected using the Hybrid Position of Barnacles and Grasshopper Algorithm (HPBGA). The enhanced model is estimated using diverse metrics in contrast with other approaches. Thus, the findings illustrate that it attains impressive results in increasing the RSS for locating the LED effectively.

**Keywords**—Visible Light Communication; RSS Maximization; Multiscale One-Dimensional Convolutional Neural Network with Symmetric Convolution; Hybrid Position of Barnacles and Grasshopper Algorithm; Mining Zones.

## I. INTRODUCTION

VLC is an innovative wireless communication technology that transmits data through visible light, utilizing the 380–750 nm region of the spectrum. In contrast to traditional radio frequency systems, VLC harnesses visible light for communication. The RSS is a crucial parameter indicating the intensity of the received light beam at a specific location, plays a pivotal role in VLC systems. The prevalence of Light-Emitting Diodes (LEDs) for illumination purposes has made VLP a viable solution for indoor applications such as location tracking, introductions, and navigation. VLP becomes particularly appealing in enclosed spaces where the Global Positioning System (GPS) is unavailable. This has garnered increased attention from both academia and industry, that leads to the development of various VLP applications. The RSS of visible light signals serves as a widely adopted measurement in several VLP techniques due to its accessibility and user-friendly nature. In the RSS-based VLP approach, LEDs function as signal sources or beacons during light

transmission. This method inversely determines the unknown User Equipment (UE) position parameters from RSS data, leveraging the propagation characteristics of visible light signals. Overall, VLC, with its reliance on visible light, presents a promising avenue for robust and efficient wireless communication, especially in indoor scenarios where traditional systems may face limitations.

One of the primary challenges faced by VLC is the attenuation of light signals as they propagate through a medium. The signal strength tends to decrease with distance due to factors like “refraction, adsorption, and dispersion”. This path loss negatively impacts the RSS and limits the communication distance of VLC systems. VLC systems predominantly rely on line-of-sight communication, necessitating an unobstructed path between the LED transmitter and the photodetector receiver. However, obstacles such as buildings and walls can obstruct the light path, leading to a decrease in RSS and potential signal blockage. Interference from ambient light sources, both artificial and natural, further complicates matters for VLC systems. Strong external light can lower the signal-to-noise ratio, impacting the accuracy and reliability of received signal strength. Additionally, visible light faces challenges in penetrating opaque materials, limiting the applicability of VLC in scenarios where communication through walls or other barriers is essential. It is crucial to understand these constraints to enhance VLC systems and develop solutions for challenges associated with Received Signal Intensity. Addressing these issues is essential for improving the performance and versatility of VLC technologies in various real-world scenarios [13][14].

Deep learning algorithms prove effective in constructing precise channel models for VLC systems. These models take into account a diverse set of environmental parameters, including room geometry, reflective surfaces and lighting properties to predict RSS in various scenarios. Predictive models enhance understanding and adaptation to the dynamic nature of VLC settings. Deep learning algorithms excel in mitigating interference and reducing noise. By training models on datasets with diverse ambient light conditions, these methods adeptly discriminate between undesired noise and VLC signals, enhancing the robustness of RSS readings. Compared to rule-based or traditional signal processing techniques, neural networks offer greater flexibility and a more sophisticated comprehension of the environment[10][11]. For a comprehensive analysis, a combination of CNN and Recurrent NN (RNN) can be employed to capture both spatial and temporal data. The quality and diversity of the training dataset significantly influence the performance of deep learning models. Ensuring adaptability, datasets should encompass a range of lighting scenarios[15], distances and environmental conditions [16]. This approach contributes to the effectiveness of deep learning models in advancing the capabilities of VLC systems.

This summarizes the primary objectives of our proposed models.

1. To create a deep learning model for maximizing the RSS in the VLC system, it aims to tackle the fundamental challenges associated with VLC and focus on elevating the quality and reliability of data transmission.
2. To design a novel deep learning architecture termed M1D-CNN-SC; this helps to elevate the accuracy and dependability of VLC systems in RSS. The parameters of the

proposed model are optimally tuned using the HPBGA algorithm to achieve optimal performance.

3. To introduce a sophisticated optimization strategy called HPBGA, which aimed at boosting the efficacy of deep learning models through precise parameter tuning and subsequently elevating their accuracy levels.

4. To analyze the outcomes of the implemented RSS maximization strategy in VLC systems compared to conventional methods, which aim to validate the performance efficacy of the proposed framework.

This study integrates a deep learning-based technique for maximizing RSS in VLC, which is detailed in the following sections. Part II reviews existing RSS maximization architectures within VLC systems. Part III introduces the VLC system and its mathematical formulation aimed at enhancing the received signal power. Part IV explores the use of MID-CNN-SC for predicting RSS maximization. Part V discusses the innovative coordinates in VLC using the hybrid position of barnacles and the grasshopper algorithm. Part VI shares the findings and insights from applying the HPBGA-based technique for RSS optimization in VLC systems. The research concludes with Part VII, summarizing the key findings and contributions of the RSS maximization approach in the context of VLC systems.

## II. LITERATURE SURVEY

### A. Related Works

In 2019, L. Bai *et al.* [1] have suggested the geometric relationships between the receiver and the LEDs were considered in the development of the channel model. The Photodiode (PD) assessed the strength of the visible light signal to determine the receiver's location using visual information. Unlike traditional RSS algorithms, the CA-RSSR method was able to alleviate the receiver-oriented restrictions by combining both visual and intensity data from visible light signals. Furthermore, compared to Perspective-N-Point (PnP) computations, which relied solely on visual data for positioning functions, the CA-RSSR demonstrated noticeably higher location accuracy. The integration of visual and intensity data contributed to improved precision in determining the receiver's position.

In 2014, Yang *et al.* [2] have recommended a single transmitter and multiple slanted optical receivers. Using the feature data obtained from this experiment, a channel link model was developed. The basis for the proposed 3-D positioning method lay in the gain distinction, which relied on both the received signal strength and the angle of reception. Through the demonstration using the collected data, it was established that the suggested algorithm had the capability to accurately determine positions including height, without being influenced by other cells.

In 2015, Gonendik and Gezici [3] have proposed the precision of distance estimation in VLP systems, focusing on range estimates derived from RSS data. Specifically, the study considered the Weighted Cramér-Rao Bound (WCRB) and Ziv-Zakai Bound (ZZB) for assessing the accuracy of RSS-based range calculations. Furthermore, Maximum A Posteriori

Probability (MAP) estimators were computed and compared with the proposed limits for RSS-based range estimation.

In 2020, Huang *et al.* [4] have suggested an advanced VLP system to simultaneously calculate the receiver frequency and transmitter position. The original estimation challenge was mathematically derived and equivalently reformulated as a location estimation problem. This involved optimizing the angle between the RSS feature vector and the received signal vector. The orientation of the RSS feature vector was identified as a one-to-one feature characterizing the position of the device receiving the signal. Notably, the proposed VLP technique demonstrated resilience to changes in transmission conditions. This was attributed to its reliance on the ratios of receiver coefficients rather than precise values of transceiver parameters, making it more robust compared to existing methods.

In 2021, Marwa *et al.* [5] have proposed a receiver positioning system, utilizing the RSS positioning method, specifically applied in low-light VLC scenarios, showcasing the technology's effectiveness in dim environments. The RSS method was chosen for indoor placement due to its user-friendly nature. This concept ensured Indoor Positioning (IP) even in "OFF" light conditions, a feature that VLC systems could employ for power conservation and precise lighting management. The gathered results indicated that, in comparison to the standard mode, the average position error induced by the LED powering the low-light VLC was diminished. This highlighted the successful implementation of the RSS positioning method in dark VLC environments.

In 2020, Ulkar *et al.* [6] have recommended the VLC net to address the limitations of practical applications in the field. Despite the growing number of neural network-based channel decoders in the scientific community, few effectively tackled these limitations. VLCnet stood out as an error rate reduction approach that aimed to maintain a specific lighting level while minimizing flicker. In pursuit of generality, our analysis took into consideration the input-dependent noise generated by the shot sound, and the Channel Impulse Response (CIR) was derived from standard CIRs for VLC. The primary innovation highlighted in this work, and a crucial component of VLCnet was the introduction of Flicker Reduction Activation Units (FRAU). FRAU serving as a competing layer, ensured run length limits for flicker mitigation, showcasing its significance in the overall framework.

In 2019, Pengfei *et al.* [7] have suggested the application of deep learning methods significantly reduced the complexity of the trilateration method, allowing the problem to be redefined as a linear mapping. This resulted in a faster location estimation process compared to traditional methods. Moreover, a novel approach to off-line preparation was employed to minimize the installation effort of the Visible Light Positioning (VLP) system, enhancing its practical usability. The proposed methodology was implemented on an atto-cellular VLP unit, facilitating the validation and demonstration of immediate performance and precision in positioning. This was evident in a 3D positioning experiment conducted in a  $1.2 \times 1.2 \times 2 \text{ m}^3$  environment, showcasing the effectiveness of the approach in a real-world setting.

In 2020, H. Lee *et al.* [8] have suggested a neural network was obtained to replace the encoder-decoder pair responsible for extracting messages from optically delivered signals, employing an uncontrolled deep learning method. To accomplish this, a collection of binary

codewords was generated from continuous-valued neural network inputs using a distinctive stochastic binarization algorithm. The deep learning-based VLC transceiver underwent training with diverse dimming constraints aiming to achieve universal support for arbitrary dimming targets. Managing such constrained training optimization proved challenging with existing deep learning approaches. A novel training technique was developed, involving a dual interpretation of the optimization process to effectively handle the dimming limitations. This innovative approach addressed the complexities associated with training optimization in the context of arbitrary dimming targets for the VLC transceiver.

Recent studies have underscored the growing relevance of VLC systems as robust communication and localization alternatives in RF-constrained industrial environments.

In 2022, Mansour *et al.* [24] investigated the deployment of VLC technology in underground mining, demonstrating its dual utility as both a lighting and wireless communication medium. The study highlighted the ability of VLC to maintain reliable data transmission in environments affected by dust and physical obstructions, which are prevalent in subsurface mining tunnels. It further emphasized the system's energy efficiency and immunity to electromagnetic interference—factors critical to safety and operational continuity in hazardous areas. Complementing this, in 2023, Zhang *et al.* [25] developed a three-dimensional VLC-based positioning system specifically tailored for underground mines, leveraging convolutional neural networks enhanced by Inception modules and attention mechanisms. Their model addressed complex challenges such as multi-path reflections and sensor tilt, significantly improving localization accuracy in dynamic and spatially constrained environments. Together, these contributions affirm the viability of VLC as a foundational communication and monitoring technology in the mining sector, while also signaling the potential for machine learning techniques to enhance system adaptability and performance in complex underground scenarios.

### B. Problem statement

When using the received signal strength approach in an indoor localization system that uses VLC, NLoS signal transmission may affect location determination accuracy. Because visible light signals can take non-direct routes, this phenomenon can result in considerable mistakes when estimating the distances between each localization node and the reference node. The challenges and features of the existing models are displayed in PnP algorithms [1] are used in computer vision to solve the Perspective-n-Point problem, which is essential in camera pose estimation. However, it is still susceptible to outliers and noise in the input data. Applications such as robotics and navigation depend on the 3-D positioning algorithm [2], which establishes the geographic location of objects in a three-dimensional space.

Nevertheless, sensor noise and ambient conditions may have an impact on accuracy. MMSE [3] is commonly used in signal processing and communication for noise reduction, but it assumes Gaussian distributions and may not perform optimally with non-Gaussian noise. RNN [4] is effective for sequence data and capturing temporal dependencies, but it is prone to vanishing/exploding gradient problems and may struggle with long-term dependencies. LED [5] is an efficient and long-lasting light source, widely used in various lighting applications, but it has limited brightness compared to other light sources. DL [6] is

powerful in learning hierarchical representations from complex data, but it requires large amounts of data and computational resources; interpretability can be a challenge. DL [7] can scale with the amount of data, and increasing data often leads to improved performance but is prone to overfitting, requires careful tuning, and may lack interpretability. For various applications, such as image identification and natural language processing, neural networks [8] are adaptable. However, because of their intricate architectures, they are frequently referred to as "black boxes" because it is challenging to understand the relationships the model has learned. These shortcomings enhance the VLC system's deep learning-based RSS.

### III. SYSTEM AND MATHEMATICAL MODEL OF VLC TO MAXIMIZE THE RECEIVED SIGNAL STRENGTH

#### A. System Model: Visible Light Communication

Indoor environments, with their enclosed spaces, floors, and ceilings, lead to reflections that can cause variations and scattering in the RSS of VLC signals [21]. These reflections are predominantly Lambertian, characterized by their diffuse scattering properties. When implementing a VLC system in practice, the dimensions of a cubic room are often considered. It's essential to ensure that external light sources like sunlight do not enter the simulation room and that the display should not be computer-generated. The setup within the room includes two distinct NLOS locations comprising one continuous receiver, which represents a user or receiving device and two LEDs functioning as transmitters. Each reflector within the room possesses a range of spectral reflectance, and their wavelength influences the rate at which they change.

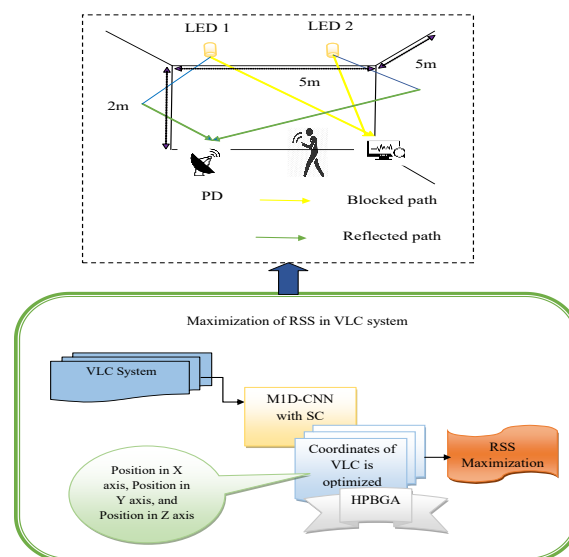


Fig 1. Structural view of recommended deep learning based RSS maximization in VLC system

This project aims to enhance the maximization of RSS by applying the newly developed HPBGA. VLC is a novel communication method that utilizes visible light with limited bandwidth for data transmission. VLC offers users multiple communication paths due to its

various light channels. A common challenge in VLC is the presence of obstacles in the communication channel or path. In such cases, the source's visible light can be reflected off surfaces and reach the receiver's PD. Obstructions along the path can lead to data transmission losses. In these situations, communication efficiency can be improved by optimizing for NLOS scenarios. The signal strength can be enhanced by selecting appropriate PD coordinates through better reflection scenarios. Fig. 1 shows the structural view of recommended deep learning-based RSS maximization in the VLC system.

This research aims to develop a deep-learning model that maximizes RSS in VLC systems. The primary goal is to improve the quality and reliability of data transmission. To this end, we propose a novel deep learning architecture named M1D-CNN-SC techniques to significantly enhance the accuracy and dependability of VLC systems in terms of RSS. The parameters of this innovative model are meticulously tuned using a sophisticated optimization strategy known as the HPBGA. The HPBGA algorithm represents a cutting-edge optimization approach designed to amplify the effectiveness of deep learning models. This is achieved through precise tuning of model parameters, which substantially improves their accuracy levels. By implementing this RSS maximization strategy within VLC systems and comparing it with traditional methodologies, our objective is to validate our proposed framework's superior performance and efficacy. This introduction lays the groundwork for a comprehensive exploration of how deep learning, specifically through the M1D-CNN model and HPBGA optimisation, can revolutionise RSS optimisation in VLC systems, setting a new standard for quality and reliability in data transmission.

### *B. Issues Related to RSS*

RSS plays a pivotal role in determining the quality and reliability of a communication link. One of the primary challenges with RSS is signal attenuation, which refers to the reduction in signal strength as it travels through different media or across distances. This attenuation can be caused by various factors such as environmental conditions, obstacles, or the sheer distance the signal must travel, resulting in a weaker signal at the receiver. Additionally, RSS can be significantly impacted by interference from other signals, particularly in frequency bands that are densely populated. This interference can come from nearby systems operating on similar frequencies or other types of electromagnetic disturbances, leading to degradation in signal quality. The effectiveness of RSS also heavily relies on the performance, quality, and design of the transmitting and receiving equipment. Variations in antenna design, orientation, and sensitivity can lead to different RSS readings even in similar environmental conditions. In mobile communication systems, RSS can experience rapid fluctuations due to user movement or changes in the surrounding environment. These dynamic changes can pose challenges in maintaining a stable and uninterrupted connection.

### *C. Mathematical Function of VLC*

Since LOS links are affected by physical obstructions, it's not feasible to use VLC through reflected light from the farthest points of a room [22]. To overcome this, NLOS communication is utilized for reliable transmission. The LED axis angle is formulated by  $\lambda_1$  and  $\lambda_2$  is defined as the angle between the LED light and the ceiling of the room. The angle of

reflected light with respect to the wall, as it reaches the PD is denoted by  $\varphi_1$ . The angle formed between the vertical axis of the room and the direction of light reflection is represented by  $\varphi_2$ . The Angle of Arrival (AOA), symbolized by  $M_{ld}$ , is the angle between the refracted light and a line parallel to the axis of the PD. The variable  $fl$  signifies the amount of transmitters and the path of LED reflection is initially described. The channel response is given by Eq. (1).

$$io^{ini}(sk, \theta_{uc}) = \int_{ih} yu_1 yu_2 E_{uc}^{ini} ret\left(\frac{\varphi_2}{EW}\right) \times \lambda\left(sk - \frac{M_{ld} + M_{pd}}{r}\right) UA_{rfl} \quad (1)$$

In Eq. (1), the specific terms  $fo$  represent various elements of the system: one term signifies the speed of light; another variable  $A_{rfl}$  represents the reflective area's surface area, followed by the FOV of the PD, the reflectance factor of the reflective surface  $cv_1$  and  $cv_2$  shows the responsivity of the PD respectively. The equation also includes a term representing the rectangular function, which accounts for the angular alignment between the light and the transmitter. In this equation, every part of a wall is assumed to be a potential reflective surface. The PD can only detect the light if both  $\varpi_1$  and  $\varpi_2$  angles are less than or equal to  $fo$ . The coefficients related to these conditions are calculated using the formulas presented in Eq. (2) and (3).

$$TR_1 = \frac{U_{rfl}(sl+1)\cos^{ha}\theta_1\cos\varphi_1}{2\pi M_{ld}^2} \quad (2)$$

The term  $ha$  in Eq. (2) denotes the directivity of light.

$$TR_2 = \frac{U_{pd}\cos\theta_2\cos\varphi_2}{\pi M_{pd}^2} \quad (3)$$

In Eq. (3), the variable  $U_{pd}$  specifies the area of PD. The function of rectangular  $RR$  is displayed in Eq. (4).

$$RR\{WQ\} = \begin{cases} 0 & |WQ| > 1 \\ 1 & |WQ| \leq 1 \end{cases} \quad (4)$$

Eq.(5) is utilized to calculate the power  $\lambda_{uc}^{ini}$  received from a single reflection.

$$\lambda_{uc}^{ini} = \int_{\eta} \theta_{uc} \varsigma_1(\chi) d\eta \quad (5)$$

In Eq. (5), the term  $\varsigma_1(\chi)$  represents the bandwidth of reflection of the reflector. Eq. (6) is used to calculate the photocurrent generated in the PD due to incident light.

$$\varphi(Er) = dr \cdot fg(Er) \otimes wq(Er) + zx(Er) \quad (6)$$

In Eq. (6), the value  $dr$ ,  $fg$  and  $wq$  represents the optical pulse carrying the noise, the PDP, and the sensitivity of the deflection. Fig 2 shows the schematic view of VLC system.

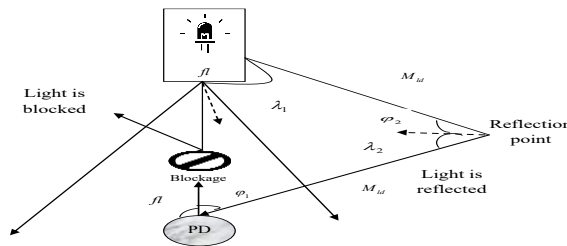


Fig. 1. Schematic view of VLC system



#### IV. PREDICTION USING MULTISCALE DEEP LEARNING MODEL WITH SYMMETRIC CONVOLUTION FOR RSS MAXIMIZATION

##### A. 1-Dimensional CNN

CNN technology has been a pivotal element in addressing complex computer vision challenges through Artificial Neural Networks (ANNs). At the core of CNNs lies the convolution process, a fundamental operation within convolution layers. Receivers field of view, transmitter location, width of room, length of room, height between transmitter and receiver, photodiode, data rate of system, amplifier current, electron charge, noise bandwidth, noise bandwidth factor, area of photodetector, area of the reflector, power emitted by LED are the initialized attributes  $R_a$ , which is fed as input to this phase. Given that these networks commonly operate on 2-dimensional images, a 2-dimensional variant of the convolution algorithm is widely employed in various computer vision applications.

The convolution involves a matrix of adjustable parameters traversing the image vertically and horizontally. This matrix scans the image, detecting visual features such as straight lines, vertical structures, and diagonal patterns. Essentially, this process enables the network to identify and capture intricate visual elements within the image, contributing to the network's ability to understand and interpret complex visual data.

In a 1-dimensional Fourier process, the primary distinctions lie in the input dimension and filter sizes, operating on the same foundational concept. This process involves a vector scan that traverses the data from top to bottom, seeking relevant features. Here,  $5 \times 1$  input vector interacts with a  $3 \times 1$  weight vector. The  $3 \times 1$  weight vector progresses in increments of 1, examining a  $3 \times 1$  section of the input at each step. This interaction results in the creation of a 3 destination vector, demonstrating the essence of the one-dimensional convolution operation.

Conventionally, a convolution resulting in an output column of size  $z$  is explained through the action of a weighted vector  $m$ , having dimensions  $u \times 1$ . This filter operates on the input vector  $E$ . This is mathematically modeled in Eq. (7).

$$s = m * E[y : y + u] R_a \quad (7)$$

The above equation represents the current position of the weight vector as it traverses the input to generate output value vectors. The weight vector is subjected to element-wise multiplication with the input, and the resulting values are subsequently summed up.

In the traditional framework, the activation layer acts on the output of the preceding convolution layer by applying a specific function element-wise to the values of the output vector. The detector utilizes the Rectified Linear Unit (ReLU) as its activation function. Apart from its computational advantages, the ReLU activation function has undergone comprehensive scrutiny and is recognized for its beneficial effects on the training process.

Following the convolution and activation layers, the dense layers, situated after the architecture, come into play. These layers operate analogously to the submerged components of conventional multi-layer perceptron systems. Regarding connectivity, the neurons within these layers are deemed "dense" due to their complete connection concerning the weights.

The thick layers within a one-dimensional CNN structure represent the final stage of parametric processes before class probabilities are generated.

### B. Proposed MID-CNN with SC for Prediction

M1D-CNN with SC represents a sophisticated approach in the field of signal processing, particularly for the task of predicting RSS.

**Multiscale:** Multiscale signal processing refers to techniques and analyses that handle signals across multiple resolutions or scales. This approach is essential for analyzing and deriving information from signals exhibiting features or patterns at different levels of detail. The core principle of multiscale signal processing is the recognition that signals often comprise information at various scales, with certain details becoming more prominent or relevant at specific scales compared to others.

**Symmetric Convolution:** Symmetric convolution is a specialized form of the standard convolution process, crucial in signal processing applications. This method involves applying a filter or kernel to a signal in a way that preserves symmetry, often leading to more desirable boundary effects for certain applications. By ensuring that the output of the convolution maintains symmetric properties, this technique plays a key role in preserving the original signal's structure. This is particularly important as asymmetry in the convolution process can introduce distortions or irregularities.

The M1D-CNN with SC model stands out with its multiscale architecture, enabling the network to capture and analyze signal features at different scales. In this proposed network, the initialized attributes  $R_a$  is the input. Integrating multiscale and SC into the traditional convolution layer of the 1DCNN is a pivotal innovation in this model. Traditional convolution methods might introduce feature extraction asymmetries, which are not ideal for VLC systems where light propagation and signal distortions can be inherently asymmetric. SC addresses this by ensuring a symmetric convolution process, leading to more accurate modeling and prediction of the RSS. By focusing on maximizing the RSS, this approach aims to significantly improve the efficiency, reliability, and applicability of VLC in various scenarios. Fig. 3 shows the proposed view of M1D-CNN with SC for prediction.

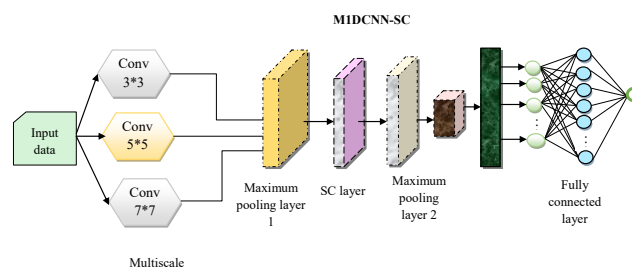


Fig. 2. Proposed view of M1D-CNN with SC for Prediction

### C. Optimal VLC Localization using Novel Algorithm

The primary mechanism for VLC localization involves triangulating a device's position based on the signal strength or the AoA of the light signals from multiple LED transmitters. The accuracy of this process is affected by various environmental factors and the inherent

limitations of the VLC system, such as in indoor environments, light signals can reflect off surfaces, creating multiple signal paths that can interfere with the direct LOS signals. Obstacles in the environment can block the direct LOS path, making it reliant on weaker reflected signals. To lessen this kind of limitation, it helps to optimize some co-ordinates like 1st position in X axis, 2nd position in Y axis and 3rd position in Z axis with the help of recommended HPBGA approach. This helps to maximize the RSS. The objective function of the proposed VLC localization system is formulated in Eq. (8).

$$Of = \arg \max_{[x_1, y_2, z_3]} [RSS] \quad (8)$$

From the above formulation, the variable  $x_1, y_2, z_3$  defines the 1st position in X axis, 2nd position in Y axis and 3rd position in Z axis. Also the term  $RSS$  specifies the received signal strength. Finally obtained the predicted outcome and which is done by M1D-CNN with SC model. Fig 4 shows the solution encoding diagram for optimal VLC localization using novel algorithm.

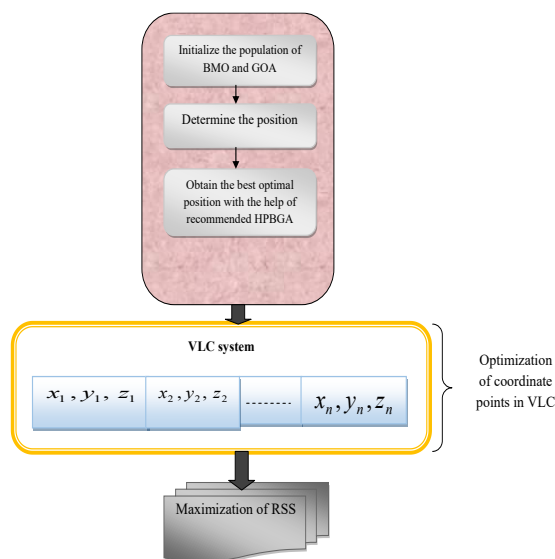


Fig. 3. Solution encoding diagram for optimal VLC localization using novel algorithm

## V. OPTIMIZING THE CO-ORDINATES IN VLC USING HYBRID POSITION OF BARNACLES AND GRASSHOPPER ALGORITHM

### A. Barnacles Mating Optimizer

Barnacles [26], ancient microorganisms dating back to the Jurassic Period, undergo a fascinating life cycle. Upon reaching adulthood, they attach themselves to various surfaces in aquatic environments and develop protective shells. Interestingly, barnacles are born with the ability to swim. A unique aspect of their reproductive strategy is that they possess both male and female reproductive organs, making the majority of them hermaphrodites. The world's rivers host a diverse array of approximately 1400 barnacle species, with acorn barnacles being the most widespread among them. What sets barnacles apart is their remarkable ability to firmly adhere underwater, achieved through the secretion of proteinaceous compounds.

**Initialization:** The proposed optimization technique assumes that barnacles offer a viable solution, and the sample vector can be expressed as following Eq. (9).

$$U = \begin{bmatrix} U_1^1 & \dots & U_1^m \\ \vdots & \ddots & \vdots \\ U_k^1 & \dots & U_k^m \end{bmatrix} \quad (9)$$

The sample size or the number of barnacles is denoted by  $m$ , and  $k$  represents the number of control factors. The upper and lower limits for the variables controlled in Eq. (10) and Eq. (11) are as follows:

$$\varphi = [\varphi_1, \dots, \varphi_i] \quad (10)$$

$$\eta = [\eta_1, \dots, \eta_i] \quad (11)$$

The variables  $\varphi$  and  $\eta$  represent the upper and lower boundaries of the  $i_{th}$  variables. The vector  $U$  is initially evaluated, and subsequently, it is sorted to identify the best answer to date, which is positioned at the top of the vector  $U$ .

**Selection process:** In the proposed BMO, the selection of two barnacles for mating is uniquely determined by the length of their genitals, setting it apart from other evolutionary algorithms such as Genetic Algorithms (GA), Differential Evolution (DE), etc.

Unlike traditional mating processes, where barnacles may choose partners beyond a certain limit, the BMO prioritizes the sperm casting phase (exploration) before offspring production. This is implemented to prevent instances where barnacles #1 that select others #8 are over the limit, hindering normal mating. It's important to note that this method operates in a virtual context and doesn't reflect the actual distances between barnacles. The process involves several straightforward choices, expressed mathematically in Eq. (12) and (13).

$$Bar\_d = Ra(m) \quad (12)$$

$$Bar\_n = Ra(m) \quad (13)$$

In this scenario,  $m$  represents the population size and the parents to be mated are denoted as  $Bar\_d$  and  $Bar\_n$ . Eq. (12) and (13) illustrate that the selection is carried out randomly, satisfying the first assumption outlined in the preceding subsection.

**Reproduction:** Unlike traditional evolution algorithms, BMO introduces a slightly different reproductive method. In this context, BMO employs the Hardy-Weinberg principle to highlight genotype frequency or inheritance characteristics of barnacle parents for offspring generation. Due to the absence of precise equations or formulas for barnacle reproduction, the following formulas are proposed to generate new offspring variables from both sets of barnacles. This theoretical model is expressed in Eq. (13) to illustrate the simplicity of the suggested BMO.

$$U_i^{m,new} = Yu_{Bar\_d}^m - Yu_{Bar\_n}^m \quad (14)$$

Sperm casting takes place when the number of barnacles selected for mating exceeds the initial  $sl$  ratio. The two equations mentioned above encapsulate the sperm casting procedure in Eq. (15).

$$Ra_i^{m,new} = Ra() \times u_{bar}^m p_1 \quad (15)$$

Where  $Ra()$  is the random number between  $[0, 1]$  and the variable  $p_1$  denotes the initiation position. Innovatively, a state-of-the-art optimization technique is set to be developed, drawing inspiration from the intricate mating process of barnacles. This new approach aims to leverage the efficient and resilient nature of barnacle adhesion for cutting-edge applications.

#### Conventional Algorithm 1: BMO

Initializing the barnacle population to zero.

Initialize the barnacles population  $U$

To filter and obtain the top outcome among the population

**While**  $i < \max_{iter}$  **do**

Assume the value of  $Pl$

Choose using Eq. (10) and Eq. (11).

**If** choice of Dad and Mum =  $sl$

**for** every variable

Off Generating offspring using Eq. (13).

**end for**

Ensuring that if a barnacle ventures beyond the borders, it is repositioned back within.

Assessing the fitness of each boundary, and reorganizing and updating if a more optimal solution exist.

Verify the position of each barnacle, correcting it if it exceeds the defined boundaries.

Evaluate the fitness of each boundary and reorganize, updating if a superior solution is identified.

Filter and upgrade  $t$  if there is better solution

$l = i + 1$

**End if**

**End While**

Return  $t$

### B. Grasshopper Optimization Algorithm

Grasshoppers [27] are classified as insects, these are considered pests due to the agricultural and crop damage they inflict. Despite their tendency to be solitary in the wild, grasshoppers exhibit one of the largest swarm formations among animals. The size of these swarms can be daunting for farmers, potentially extending to continental proportions. Upon reaching adulthood, they take to the air as a swarm, covering great distances. The following Eq. (16) constitutes the mathematical framework used to simulate the behavior of hopper swarms.

$$U_i = K_i + J_i + M_i \quad (16)$$

In this context, the statement  $U_i, K_i, J_i$  delineates the  $i_{th}$  grasshopper's position, social interactions, gravitational pull on the grasshopper and the influence of wind, a process referred to as  $M_i$ . It is important to highlight that the formula can be represented as  $U_i = RaK_i + RaJ_i + RaM_i$ , where  $Ra$  signifies random numbers within the range  $[0, 1]$  to induce stochastic behavior.

The  $J$  function that defines the societal forces is calculated using the formula given by Eq. (17).

$$J(Ra) = Le^t - e^t \quad (17)$$

The variable  $L$  representing the degree of attraction in this context  $e$  is the appealing length scale. The computation  $M$  of the element in Eq. (18) is expressed as follows:

$$M = -me_i \quad (18)$$

Here,  $R$  denotes a unity vector pointing toward the Earth's center and  $me_i$  is the gravitational constant. The computation  $E$  of the element in Eq. (19) is determined as follows:

$$E_i = Ie_w \quad (19)$$

In this instance, the term  $I$  signifies a consistent movement and the vector  $Ie_w$  symbolizes unity in the wind direction. Given that nymph grasshoppers lack wings, the wind direction plays a crucial role in influencing their movements, which is displayed in Eq. (20).

$$U_i = \sum_{j=1}^m k(|u_j - u_i|) \frac{u_j - u_i}{h_{i,j}} - e_i + Ie_w \quad (20)$$

To prevent nymph grasshoppers from settling on the ground, they need to be kept below a certain threshold. However, because including this equation would hinder the algorithm from exploring and utilizing the search space around a solution, it will be excluded from the swarm optimization and simulation process. In reality, the swarm model operates in free space.

Unfortunately, the mathematical model cannot be directly applied to address optimization issues as the swarm fails to converge to a predetermined point and the grasshoppers rapidly expand their comfort zone. To address optimization problems, a modified version of this equation is proposed, demonstrated mathematically in Eq. (21):

$$U_i^d = \left( \sum_{j=1}^m k \frac{\phi - \eta}{2} (|u_j - u_i|) \frac{u_j - u_i}{h_{i,j}} \right) + Ie_w \quad (21)$$

As the number of iterations increases, this mechanism promotes exploitation. The coefficient  $L$ , determined by the following Eq. (22), decreases the comfort zone based on the number of iterations.

$$L = L_{\max} - p_2 \frac{L_{\max} - L_{\min}}{L} \quad (22)$$

In this context, the values  $L_{\max}$ ,  $L_{\min}$ ,  $L$  and  $L_s$  correspond to the highest, least, current, and maximum number of iterations respectively. Also the variable  $p_2$  defines the second position.

### Conventional Algorithm 2: GOA

Begin GOA

Initialize the Swarm

Determine the fitness of each search agent

**While**  $i < \max_{iter}$  **do**

**Upgrade**  $L$  **using** Eq.(22)

**for** every search agent

Adjust the spacing between grasshoppers to normal.

The Eq. (21) is employed to elevate the current search agent's position.

If the current search agent crosses any boundaries, please reposition it within the defined limits.

**end for**

Upgrade  $t$ , if there is a better solution

$i = i + 1$

**End while**

Return  $t$

### C. Novel Hybrid Algorithm: HPBGA

This designed HPBGA has helped to achieve an optimal VLC technique. This developed HPBGA method is an evolution of the well-known BMO [26] and GOA [27] technique. There are diverse heuristic algorithms such as Genetic Algorithm (GA), Particle Swarm Optimization (PSO), Ant Colony Optimization (ACO), and so on, which have been developed for resolving optimization problems. However, selecting the proper heuristic algorithm is important because it directly influences the accuracy and efficiency of resolving complex issues. The proper selection of algorithms enables the rapid discovery of 'good

enough' outcomes. By considering this context, the developed model analyzes the distinct algorithms. The GA resolves complex issues and generates novel solutions.

However, the convergence of the GA is relatively slow. The PSO has fast convergence and is simple to develop. However, the PSO easily fell into the local optima. The ACO performs parallel computation and applies to distinct issues. However, this algorithm also faces suboptimal issues and computational complexity. The BMO is a bio-inspired algorithm designed to resolve optimization issues. It has high efficiency and reliability. Moreover, the convergence rates of this algorithm are high. The BMO is also a straightforward algorithm with fewer parameters. Moreover, the GOA is another optimization algorithm. This algorithm helps find the optimal solutions and applies to distinct optimization issues. The GOA is efficient in rectifying the global unconstrained and constrained optimization issues. These two algorithms are considered in this work by focussing on these significant merits. However, the BMO's risk of falling into the local optimum is higher, and the GOA's convergence is lower. Therefore, individually processing these two algorithms may hinder exploring optimal solutions. To prevent these limitations, these two algorithms are combined.

**Novelty:** The developed HPBGA combines the merits of both BMO and GOA. Moreover, it resolves the problems in these algorithms. By integrating these two algorithms, a specialized method has been proposed. This method focuses on minimizing errors, aiming to mitigate the limitations and improve the effectiveness of the HPBGA approach. An improved position is introduced for the HPBGA. This position  $P_s$  of the recommended framework is mathematically represented by Eq. (23).

$$P_s = \frac{O_p + st(p_1, p_2)}{100} \quad (23)$$

From the above formulation, the terms  $O_p$  and  $st$  define the old position and standard deviation. Also the variables  $p_1$  and  $p_2$  specify the initial and second positions. In this scenario, two separate updates are specified:  $p_1$  and  $p_2$ . Here, the updated position of BMO is specified as  $p_1$ , while  $p_2$  is updated position of GOA.

Though there are distinct models that have been implemented for optimizing the VLC, the existing optimization mechanisms struggle to manage the fluctuations of light intensity, guarantee convergence in complex scenarios, handle the data rate with less power usage, and resolve the interference from ambient light. In order to resolve these issues, the HPBGA is implemented. This HPBGA efficiently resolves these issues by optimizing the coordinates that make the system highly effective. The suggested HPBGA helps to maximize the RRS and thus recognizes the optimal coordinates for the receiver of the Photo Detector (PD).

#### ***The steps of developed HPBGA for optimizing the coordinates:***

The recommended HPBGA mainly focuses on a significant position, which is derived by the BMO and GOA. The developed HPBGA helps to discover the appropriate coordinates  $x_1, y_2$ , and  $z_3$  for the PD from the random coordinates and upgrades the solutions according to the fitness validated for the present solution. At the end of the iteration, the coordinates of PD are optimally selected. The steps for developing HPBGA-based coordinate optimization of receiver PD are provided as follows.



**Initialization:** Initially, the receiver PD coordinates are selected randomly. Further, the population of barnacles and swarms is initialized. The coordinates are then encoded in the populations.

**Fitness evaluation:** The fitness value is estimated for each random value. It is one of the significant steps in the optimization. The developed HPBGA utilizes the fitness values for finding the suitable coordinates. In Eq. (8), the fitness value is estimated. As explained in the fitness function  $Of$ , the solution must obtain the RSS rates to improve the VLC's effectiveness. In this, the fitness value is processed via the RSS value maximization thus the solution coordinates having the maximum fitness value is referred to as the best outcome.

**Position updating of BMO:** In the BMO, the barnacle's new offspring is produced. In each iteration, the best outcomes obtained so far are upgraded, which is positioned at the vector's top. To handle the matrix enlargement from the population size, each barnacle's new offspring is validated and connected with its parents. From this phase, the sorting operation is conducted to choose the half of the top solution that fits the size of the population. Finally, the updated position is specified as  $p_1$ .

**Position updating of GOA:** In the GOA, the search agents upgrade their positions. The best target positions acquired so far are upgraded in each iteration. Moreover, in each iteration, the distances among the grasshoppers are normalized. Iteratively, the position updating is carried out until a satisfactory solution is achieved. The best target's fitness and position are returned as the final solutions. The updated position is indicated as  $p_2$ .

**Formulate the adaptive concept:** The developed HPBGA introduces an adaptive mechanism for hybridizing the existing BMO and GOA. Here, a new position is formulated, where the positions of BMO and GOA are employed. This improved position helps to resolve the local optimum issue and obtains fast convergence. Moreover, the model becomes more effective than the other existing single heuristic algorithms. Based on Eq. (23), this newly derived position  $P_s$  is updated.

**Finding a global best solution:** Based on Eq. (23), a new position  $P_s$  is updated by considering the positions of BMO and GOA, and then the solution's fitness is again validated. And the solution with the maximized value of RSS is considered as the global best coordinates.

**Termination:** The algorithm processes the iteration from  $i$  to  $I_{iter}$ . At the end of the iteration, the best solution coordinates are obtained. Thus, the optimal coordinates  $x_1, y_2$ , and  $z_3$  for the PD are achieved for receiving the signal.

Fig. 5 shows the flowchart of the recommended HPBGA approach. The pseudo-code of the proposed system is displayed below.

Recommended Algorithm 3: HPBGA
<b>Input:</b> Randomly selected coordinates of PD
<b>Output:</b> Optimized coordinates of PD
Initialize the population of BMO and GOA
Determine the fitness of each search agent

For  $i=1$  to  $I_{iter}$

For  $u=1$  to  $U$

**Perform BMO**

Ensuring that if a barnacle ventures beyond the borders, it is repositioned back

Assessing the fitness of each boundary, and reorganize and update if a more optimal solution exists

Verify the position of each barnacle, and adjust it if it exceeds the defined boundaries

Evaluate the fitness of each boundary and reorganize, update if a superior solution is identified

Upgrade the position  $p_1$  using Eq. (15)

**Perform GOA**

Adjust the spacing between grasshoppers to normal

Eq. (21) is employed to elevate the current search agent's position

If the current search agent crosses any boundaries, please reposition it within the defined limits

Upgrade the position  $p_2$  using Eq. (22)

**End for**

**Update the parameter  $P_s$  with a newly developed concept in Eq. (23)**

Save the best solution

**End for**

Return optimal solution

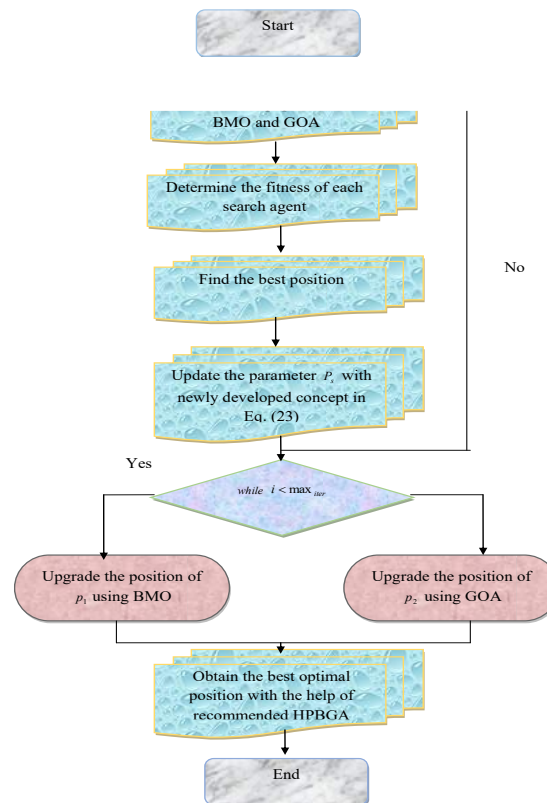


Fig. 4. Flowchart view of recommended HWSBIA approach

## VI. RESULTS AND DISCUSSION

### A. Simulation setup

The method for maximizing the RSS in VLC through deep learning was developed and validated using the powerful numerical computing environment, MATLAB. This platform offered several advantages in terms of data visualization. The performance results were compared against those obtained using classifier-based approaches such as Resnet [17], Inception-v3 [18], Xception [19], 1D-CNN + RNN [20], as well as traditional algorithms like the Reptile Search Algorithm (RSA)-M1D-CNN-SC [11], Eurasian Oystercatcher Optimizer (EOO)-M1D-CNN-SC [12], Butterfly Optimization Algorithm (BMO)-M1D-CNN-SC [9], and Grasshopper Optimization Algorithm (GOA)-M1D-CNN-SC [12].

### B. Cost function evaluation

Fig. 6 presents the outcomes of assessing the cost function for the proposed deep learning strategy aimed at maximizing RSS in VLC. This approach is compared to traditional algorithms to evaluate its cost-effectiveness. According to the results, over a span of 50 iterations, the proposed secure H-HPBGA-M1D-CNN-SC technique exhibited a reduction in cost value by 12.5%, 30%, 41.66%, and 53.33% compared to RSA-M1D-CNN-SC, EOO-M1D-CNN-SC, BMO-M1D-CNN-SC, and GOA-M1D-CNN-SC, respectively. These findings underscore the cost-efficiency of the proposed method over traditional alternatives.

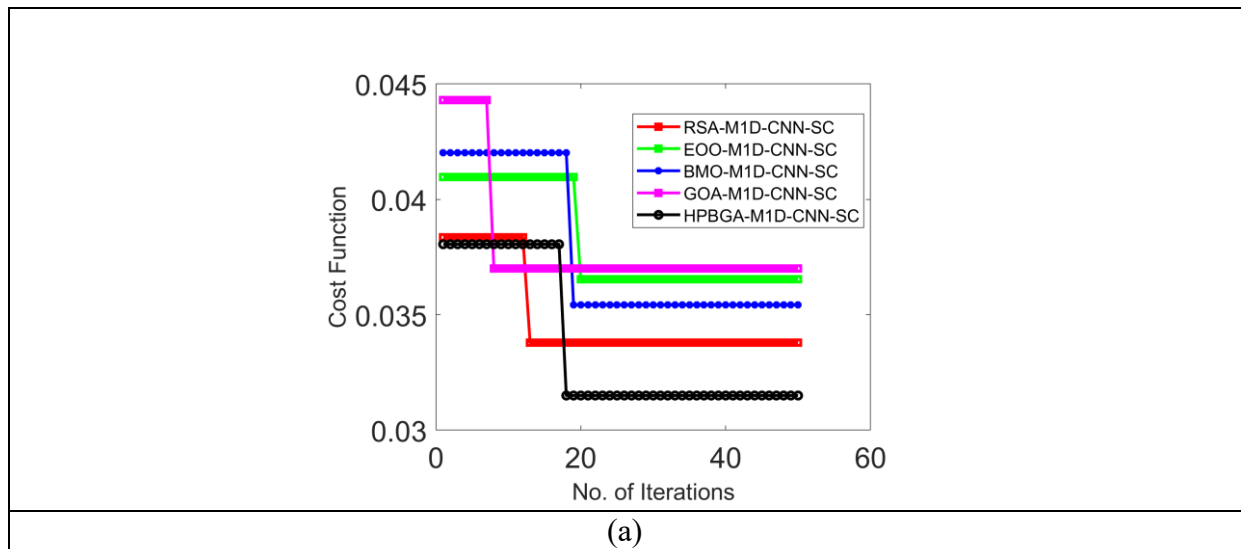
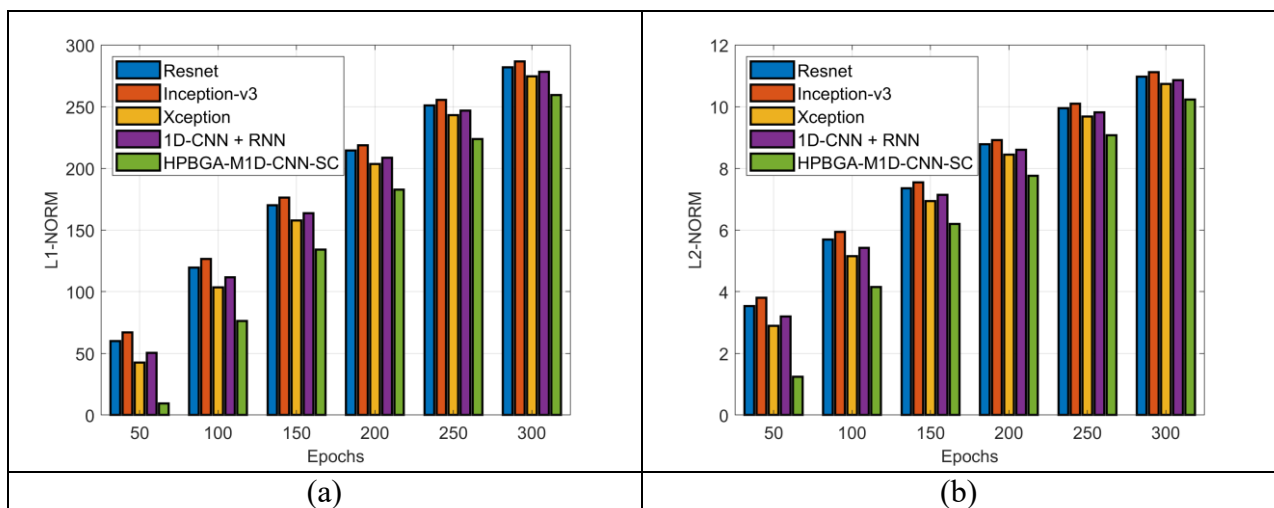


Fig. 5. Cost function examination results of the recommended maximizing the RSS in VLC system over the traditional algorithms

### C. Error comparison over the traditional algorithms and classifier

Fig. 7 and 8 illustrates a comparison of error rates between the current classifier and various algorithms. Fig. 7(d) reveal that, over 300 epochs, the MAE for the proposed method is lower than that of RSA-M1D-CNN-SC, EOO-M1D-CNN-SC, BMO-M1D-CNN-SC, and GOA-M1D-CNN-SC by 2.26%, 10%, 54.44%, and 23.33%, respectively. These results confirm the lower MAE of the proposed approach.



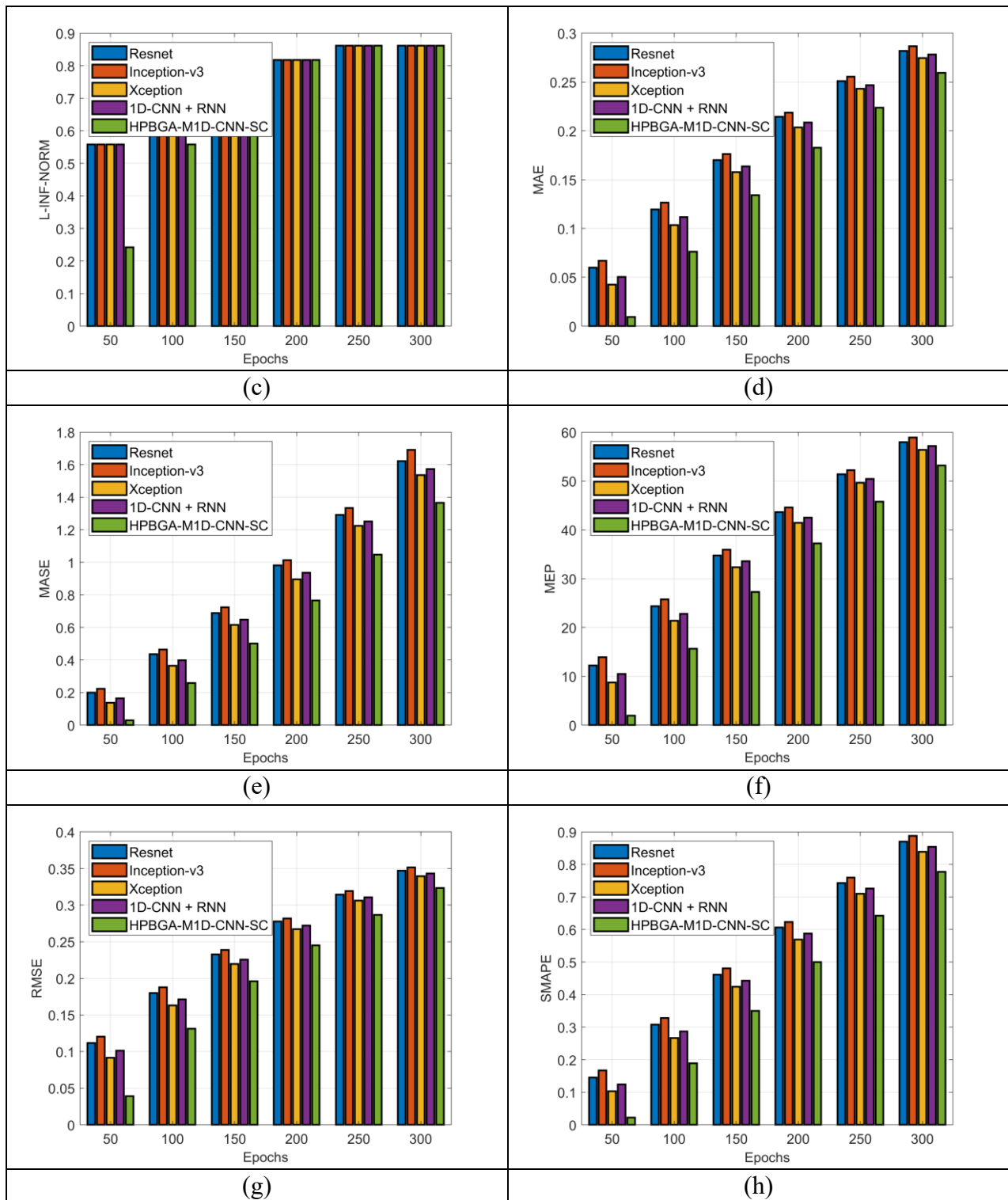
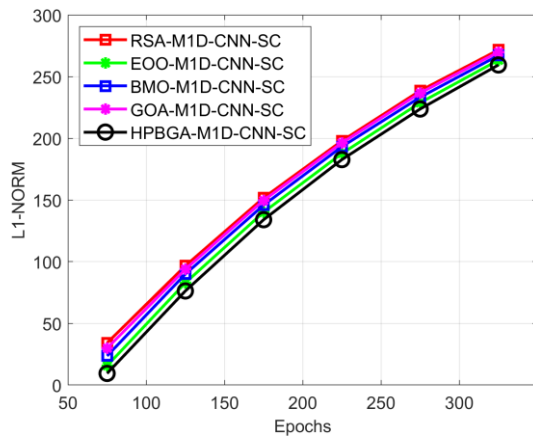
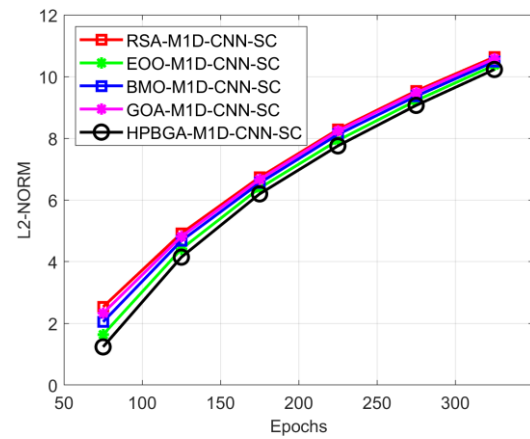


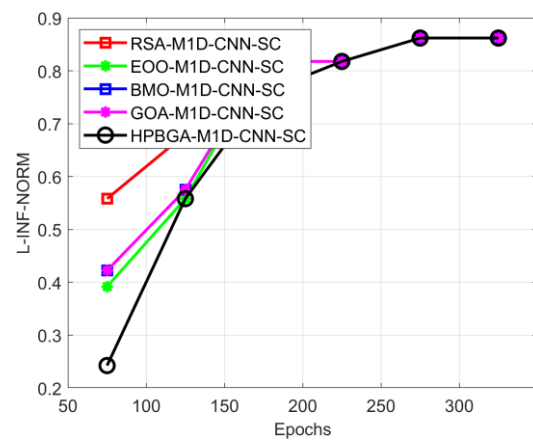
Fig. 6. Error comparison of the recommended maximizing the RSS in VLC through deep learning over the prior classifier concerning “(a) L1-Norm (b) L2-Norm (c) L-Inf-Norm (d) MAE (e) MASE (f) MEP, (g),RMSE and (h)SMAPE”



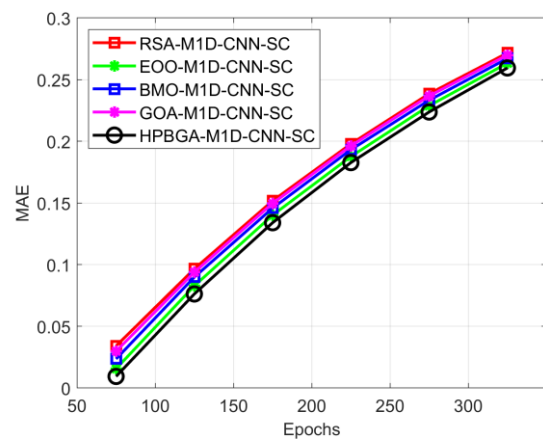
(a)



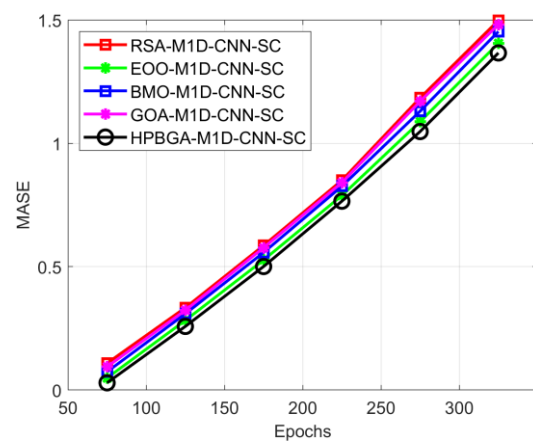
(b)



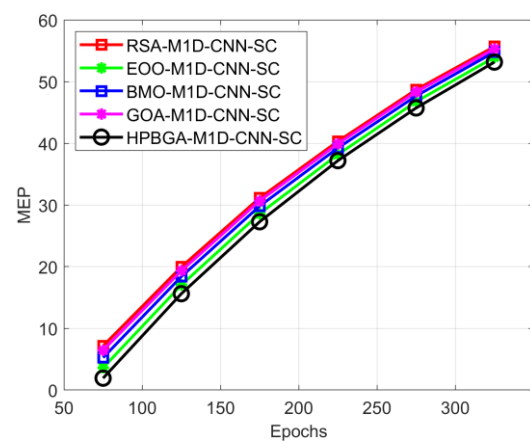
(c)



(d)



(e)



(f)

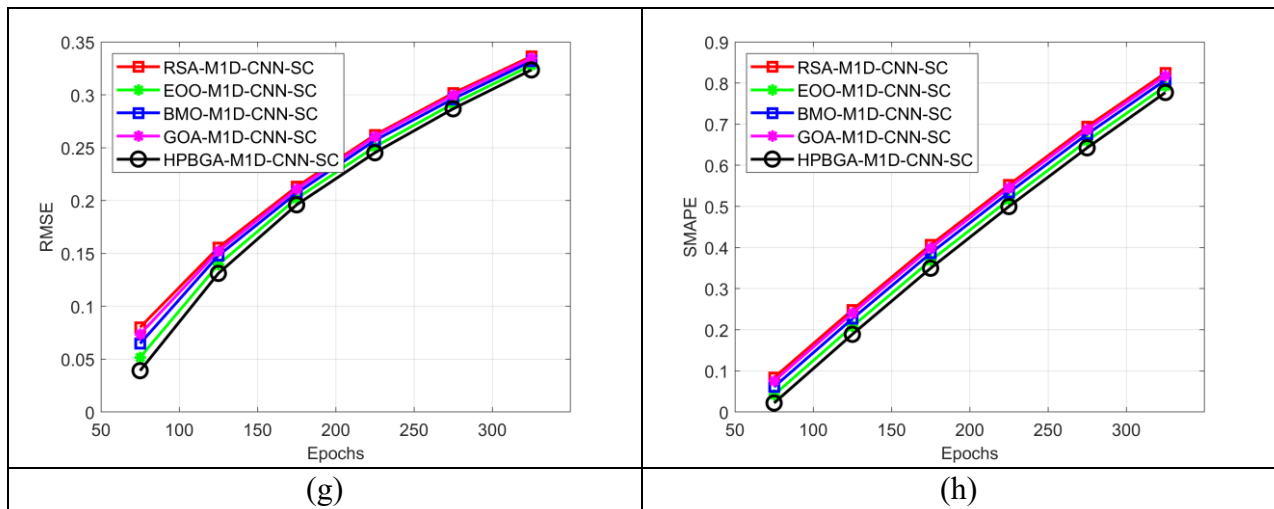


Fig. 7. Error comparison of the recommended maximizing the RSS in VLC through deep learning over the prior algorithm concerning “(a) L1-Norm (b) L2-Norm (c) L-Inf-Norm (d) MAE (e) MASE (f) MEP, (g) RMSE and (h) SMAPE”

#### D. Power comparison over the width and length of the room

Fig. 9 illustrates a power comparison over the width and length of the room. This involves analyzing how the power of the transmitted light signal changes as it travels over the width and length of an indoor environment. This comparison is essential for ensuring reliable data transmission, this helps to minimizing dead zones and achieving uniform coverage throughout the space.

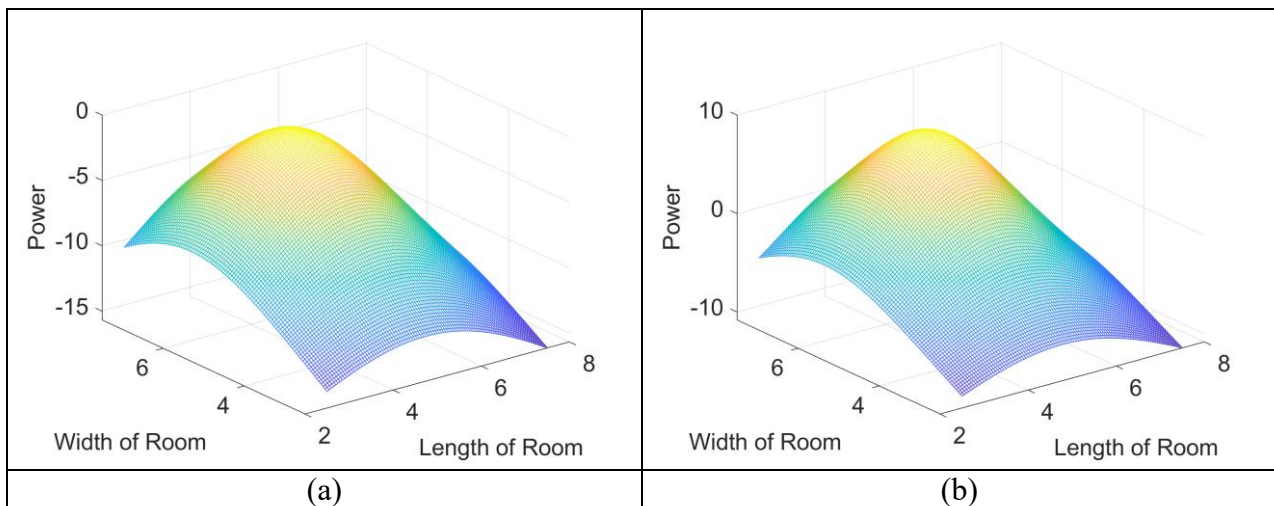


Fig. 8. Power comparison over the width and length of the room concerning (a) Configuration 1 and (b) Configuration 2

#### E. Statistical analysis outcomes of the recommended algorithm

Table II showcases the outcomes of the statistical evaluation for the deep learning-based method aimed at enhancing RSS in VLC, in contrast to conventional strategies. The data demonstrates that, relative to RSA-M1D-CNN-SC, EOO-M1D-CNN-SC, BMO-M1D-CNN-SC, and GOA-M1D-CNN-SC, the developed approach recorded superior average

improvements of 22.22%, 20.18%, 9.09%, and 31.37%, respectively. These results affirm that the proposed offloading strategy outperforms existing models in terms of efficiency.

TABLE I.  
STATISTICAL EVALUATION OUTCOMES OF THE RECOMMENDED DEEP  
LEARNING BASED MAXIMIZATION OF RSS IN VLC OVER THE CONVENTIONAL ALGORITHMS

Terms	RSA-M1D- CNN-SC [28]	EOO-M1D- CNN-SC [29]	BMO-M1D- CNN-SC [26]	GOA-M1D- CNN-SC [27]	HPBGA- M1D-CNN- SC
“Best”	0.033796	0.036539	0.035432	0.0315	0.033796
“Worst”	0.038355	0.040963	0.042025	0.038054	0.038355
“Mean”	0.03489	0.03822	0.037805	0.033728	0.03489
“Median”	0.033796	0.036539	0.035432	0.0315	0.033796
“Standard deviation”	0.001967	0.002169	0.0031968	0.003136	0.001967

*F. Validation using various measures concerning both the algorithm and classifier for the developed model*

In Table III and Table IV, the validation has been carried out using diverse performance measures in terms of both the algorithm and classifier model for estimating the performance of developed deep learning-based RSS maximization in VLC. Here, distinct error measures are considered, where the performance is analyzed by varying the epoch sizes. The epoch size-assisted validation supports to assess the implemented process effectively. When considering the 200<sup>th</sup> epoch value, the suggested mechanism’s MEP is minimized by 8.43% of RSA-M1D-CNN-SC, 2.65% of EOO-M1D-CNN-SC, 5.5% of BMO-M1D-CNN-SC, and 7.33% of GOA-M1D-CNN-SC. Here, this experiment ensures that the implemented deep learning strategy is highly supported in maximizing the RSS than the existing algorithms and methods.

TABLE II.  
OVERALL ANALYSIS FOR THE PROPOSED DEEP LEARNING BASED  
MAXIMIZATION OF RSS IN VLC OVER ALGORITHMS

Epoch sizes	RSA-M1D- CNN-SC [28]	EOO-M1D- CNN-SC [29]	BMO-M1D- CNN-SC [26]	GOA-M1D- CNN-SC [27]	HPBGA- M1D-CNN- SC
<b>MEP</b>					
<b>50</b>	7.1656	3.6188	5.2578	6.4578	1.925
<b>100</b>	19.972	17.031	18.398	19.338	15.623
<b>150</b>	31.15	28.592	29.819	30.673	27.28
<b>200</b>	40.333	38.185	39.244	39.92	37.193
<b>250</b>	48.703	46.761	47.679	48.33	45.735
<b>300</b>	55.683	53.942	54.787	55.313	53.168
<b>SMAPE</b>					
<b>50</b>	0.083878	0.041897	0.061202	0.075396	0.022
<b>100</b>	0.24852	0.20819	0.22697	0.24023	0.18908



<b>150</b>	0.40656	0.36834	0.3862	0.3989	0.34976
<b>200</b>	0.55258	0.51635	0.53369	0.54537	0.49978
<b>250</b>	0.69432	0.65974	0.67583	0.68745	0.64254
<b>300</b>	0.82445	0.7922	0.80737	0.81767	0.77714
<b>MASE</b>					
<b>50</b>	0.10894	0.049085	0.074113	0.094502	0.029371
<b>100</b>	0.33389	0.28237	0.30912	0.32317	0.258
<b>150</b>	0.58601	0.52712	0.55753	0.57678	0.50076
<b>200</b>	0.8501	0.78844	0.82591	0.84066	0.76558
<b>250</b>	1.1842	1.0883	1.1303	1.17	1.0478
<b>300</b>	1.4982	1.4058	1.4531	1.4815	1.3663
<b>MAE</b>					
<b>50</b>	0.034125	0.015688	0.023616	0.029845	0.0094279
<b>100</b>	0.096636	0.082854	0.089931	0.093858	0.076275
<b>150</b>	0.15178	0.14014	0.14587	0.14969	0.13404
<b>200</b>	0.19792	0.18766	0.19319	0.1963	0.18275
<b>250</b>	0.23859	0.22884	0.2333	0.23674	0.22377
<b>300</b>	0.27164	0.26336	0.26715	0.26991	0.25948
<b>RMSE</b>					
<b>50</b>	0.080169	0.051706	0.064796	0.073685	0.039141
<b>100</b>	0.15556	0.13955	0.1479	0.15227	0.13115
<b>150</b>	0.21307	0.20197	0.20717	0.21082	0.19601
<b>200</b>	0.26202	0.25088	0.25689	0.26047	0.24524
<b>250</b>	0.30155	0.29165	0.29622	0.29973	0.28678
<b>300</b>	0.33632	0.32797	0.33168	0.33462	0.32359
<b>L1-NORM</b>					
<b>50</b>	34.125	15.688	23.616	29.845	9.4279
<b>100</b>	96.636	82.854	89.931	93.858	76.275
<b>150</b>	151.78	140.14	145.87	149.69	134.04
<b>200</b>	197.92	187.66	193.19	196.3	182.75
<b>250</b>	238.59	228.84	233.3	236.74	223.77
<b>300</b>	271.64	263.36	267.15	269.91	259.48
<b>L2-NORM</b>					
<b>50</b>	2.5352	1.6351	2.049	2.3301	1.2377
<b>100</b>	4.9192	4.4131	4.677	4.8151	4.1472
<b>150</b>	6.7379	6.387	6.5513	6.6669	6.1982
<b>200</b>	8.2858	7.9334	8.1237	8.2368	7.755
<b>250</b>	9.5359	9.2227	9.3673	9.4782	9.0687
<b>300</b>	10.636	10.371	10.489	10.582	10.233
<b>L-INF-NORM</b>					
<b>50</b>	0.55819	0.39191	0.42241	0.42241	0.24257
<b>100</b>	0.68003	0.55819	0.57511	0.57511	0.55819

<b>150</b>	0.81774	0.81774	0.81774	0.81774	0.75872
<b>200</b>	0.81774	0.81774	0.81774	0.81774	0.81774
<b>250</b>	0.862	0.862	0.862	0.862	0.862
<b>300</b>	0.862	0.862	0.862	0.862	0.862

TABLE III.

OVERALL ANALYSIS FOR THE PROPOSED DEEP LEARNING BASED  
MAXIMIZATION OF RSS IN VLC OVER CLASSIFIERS

<b>Epoch sizes</b>	<b>Resnet [30]</b>	<b>Inception [31]</b>	<b>Exception [32]</b>	<b>1DCNN+RNN [33]</b>	<b>HPBGA-M1D-CNN-SC</b>
<b>MEP</b>					
<b>50</b>	8.7609	10.462	12.246	13.925	1.925
<b>100</b>	21.358	22.784	24.346	25.756	15.623
<b>150</b>	32.329	33.545	34.742	35.948	27.28
<b>200</b>	41.41	42.519	43.627	44.603	37.193
<b>250</b>	49.612	50.447	51.358	52.231	45.735
<b>300</b>	56.394	57.178	57.946	58.91	53.168
<b>SMAPE</b>					
<b>50</b>	0.10334	0.12391	0.14563	0.16735	0.022
<b>100</b>	0.26713	0.28667	0.30762	0.32824	0.18908
<b>150</b>	0.4242	0.44294	0.46142	0.48038	0.34976
<b>200</b>	0.56931	0.58746	0.60615	0.62318	0.49978
<b>250</b>	0.71013	0.72626	0.74305	0.75968	0.64254
<b>300</b>	0.83873	0.85439	0.87019	0.88795	0.77714
<b>MASE</b>					
<b>50</b>	0.13716	0.16381	0.19961	0.22303	0.029371
<b>100</b>	0.36427	0.39908	0.4349	0.46466	0.258
<b>150</b>	0.6166	0.6475	0.68766	0.72442	0.50076
<b>200</b>	0.89603	0.93584	0.98246	1.0145	0.76558
<b>250</b>	1.2246	1.2511	1.2912	1.3336	1.0478
<b>300</b>	1.5356	1.5733	1.623	1.6911	1.3663
<b>MAE</b>					
<b>50</b>	0.04258	0.050374	0.060077	0.066919	0.0094279
<b>100</b>	0.10363	0.11159	0.11955	0.12644	0.076275
<b>150</b>	0.15768	0.16369	0.17019	0.17615	0.13404
<b>200</b>	0.20361	0.20869	0.21451	0.2188	0.18275
<b>250</b>	0.24319	0.24687	0.25108	0.25543	0.22377
<b>300</b>	0.27469	0.27836	0.2819	0.28662	0.25948
<b>RMSE</b>					
<b>50</b>	0.091611	0.10119	0.11183	0.12024	0.039141
<b>100</b>	0.16305	0.17143	0.17987	0.18795	0.13115
<b>150</b>	0.21952	0.2257	0.23273	0.23875	0.19601
<b>200</b>	0.2671	0.27193	0.27781	0.28194	0.24524

<b>250</b>	0.30623	0.31049	0.31457	0.31929	0.28678
<b>300</b>	0.33958	0.34339	0.34712	0.3515	0.32359
<b>L1-NORM</b>					
<b>50</b>	42.58	50.374	60.077	66.919	9.4279
<b>100</b>	103.63	111.59	119.55	126.44	76.275
<b>150</b>	157.68	163.69	170.19	176.15	134.04
<b>200</b>	203.61	208.69	214.51	218.8	182.75
<b>250</b>	243.19	246.87	251.08	255.43	223.77
<b>300</b>	274.69	278.36	281.9	286.62	259.48
<b>L2-NORM</b>					
<b>50</b>	2.897	3.2	3.5365	3.8022	1.2377
<b>100</b>	5.156	5.4212	5.6881	5.9435	4.1472
<b>150</b>	6.9417	7.1372	7.3595	7.55	6.1982
<b>200</b>	8.4466	8.599	8.785	8.9159	7.755
<b>250</b>	9.684	9.8185	9.9474	10.097	9.0687
<b>300</b>	10.739	10.859	10.977	11.115	10.233
<b>L-INF-NORM</b>					
<b>50</b>	0.55819	0.55819	0.55819	0.55819	0.24257
<b>100</b>	0.68003	0.68003	0.75872	0.75872	0.55819
<b>150</b>	0.81774	0.81774	0.81774	0.81774	0.75872
<b>200</b>	0.81774	0.81774	0.81774	0.81774	0.81774
<b>250</b>	0.862	0.862	0.862	0.862	0.862
<b>300</b>	0.862	0.862	0.862	0.862	0.862

## VII. CONCLUSION

This research paper developed a deep learning model dedicated to maximizing RSS in VLC systems, aiming to improve the quality and reliability of data transmission. To this end, a novel deep learning architecture named MID-CNN-SC techniques was proposed. The parameters of this innovative model were meticulously tuned using a sophisticated optimization strategy known as the HPBGA. The HPBGA algorithm represented a cutting-edge approach to optimization designed to amplify the effectiveness of deep learning models. By implementing this RSS maximization strategy within VLC systems and comparing it with traditional methodologies, the objective was to validate the superior performance and efficacy of the proposed framework. The MASE for the proposed method was lower than that of RSA-MID-CNN-SC, EOO-MID-CNN-SC, BMO-MID-CNN-SC, and GOA-MID-CNN-SC by 226%, 20%, 54.44%, and 73.33%, respectively. These results confirm the superior accuracy of the proposed approach. The proposed model's ability to handle interference from ambient light sources and other nearby VLC systems has been less explored. This factor is critical for the robustness of VLC systems in real-world applications. Incorporating mechanisms for better handling of interference from both ambient light and other VLC systems can improve the robustness and reliability of the proposed RSS maximization strategy.

**References**

- [1] L. Bai, Y. Yang, C. Guo, C. Feng and X. Xu, "Camera Assisted Received Signal Strength Ratio Algorithm for Indoor Visible Light Positioning," *IEEE Communications Letters*, vol. 23, no. 11, pp. 2022-2025, Nov. 2019.
- [2] S. -H. Yang, H. -S. Kim, Y. -H. Son and S. -K. Han, "Three-Dimensional Visible Light Indoor Localization Using AOA and RSS With Multiple Optical Receivers," *Journal of Lightwave Technology*, vol. 32, no. 14, pp. 2480-2485, 1 July 2014.
- [3] E. Gonendik and S. Gezici, "Fundamental Limits on RSS Based Range Estimation in Visible Light Positioning Systems," *IEEE Communications Letters*, vol. 19, no. 12, pp. 2138-2141, Dec. 2015.
- [4] N. Huang, C. Gong, J. Luo and Z. Xu, "Design and Demonstration of Robust Visible Light Positioning Based on Received Signal Strength," *Journal of Lightwave Technology*, vol. 38, no. 20, pp. 5695-5707, 15 Oct. 2020.
- [5] Marwa M. El Gamal, R. Maheswar, Heba A. Fayed, Moustafa H. Aly, Nour Eldin Ismail and Amr Mokhtar " Dark light visible light communication positioning system with received signal strength technique", *Optical and Quantum Electronics* ,Vol. 53, article No. 542, 2021.
- [6] M. G. Ulkar, T. Baykas and A. E. Pusane, "VLCnet: Deep Learning Based End-to-End Visible Light Communication System," *Journal of Lightwave Technology*, vol. 38, no. 21, pp. 5937-5948, 1 Nov. 2020.
- [7] Pengfei Du; Sheng Zhang; Chen Chen; Helin Yang; Wen-De Zhong., "Experimental Demonstration of 3D Visible Light Positioning Using Received Signal Strength With Low-Complexity Trilateration Assisted by Deep Learning Technique," *IEEE Access*, vol. 7, pp. 93986-93997, 2019.
- [8] H. Lee, T. Q. S. Quek and S. H. Lee, "A Deep Learning Approach to Universal Binary Visible Light Communication Transceiver," *IEEE Transactions on Wireless Communications*, vol. 19, no. 2, pp. 956-969, Feb. 2020.
- [9] Mohd Herwan Sulaiman, Zuriani Mustaffa, Mohd Mawardi Saari, and Hamdan Daniyal, "Barnacles Mating Optimizer: A new bio-inspired algorithm for solving engineering optimization problems", *Engineering Applications of Artificial Intelligence*, vol. 87, January 2020,
- [10] Durairaj, S., Umar, M.M. and Natarajan, B., Evaluation of Bio-Inspired Algorithm-based Machine Learning and Deep Learning Models. In *Bio-inspired Algorithms in Machine Learning and Deep Learning for Disease Detection* (pp. 48-69). CRC Press.
- [11] Krishnan, R. and Durairaj, S., 2024. Reliability and performance of resource efficiency in dynamic optimization scheduling using multi-agent microservice cloud-fog on IoT applications. *Computing*, 106(12), pp.3837-3878.
- [12] Shahrzad Saremi, Seyedali Mirjalili and Andrew Lewis, " Grasshopper Optimization Algorithm: Theory and application", *Advances in Engineering Software*, vol. 105 , pp. 30–47, 2017.

- [13] Z. Elgamal, A. Q. M. Sabri, M. Tubishat, D. Tbaishat, S. N. Makhadmeh and O. A. Alomari, "Improved Reptile Search Optimization Algorithm Using Chaotic Map and Simulated Annealing for Feature Selection in Medical Field," *IEEE Access*, vol. 10, pp. 51428-51446, 2022
- [14] M. McBlain, K. A. Jones and G. Shannon, "Sleeping Eurasian oystercatchers adjust their vigilance in response to the behaviour of neighbours, human disturbance and environmental conditions", *Journal of Zoology*, 29 May 2020.
- [15] Durairaj, S., S, S. and S, A.A.B., 2025. Hybrid key management WSN protocol to enhance network performance using ML techniques for IoT application in cloud environment. *Peer-to-Peer Networking and Applications*, 18(4), p.163.
- [16] Durairaj, S. and Sridhar, R., 2024. Coherent virtual machine provisioning based on balanced optimization using entropy-based conjectured scheduling in cloud environment. *Engineering Applications of Artificial Intelligence*, 132, p.108423.
- [17] Y. Fan, J. Shao, G. Sun and X. Shao, "A Self-Adaption Butterfly Optimization Algorithm for Numerical Optimization Problems," *IEEE Access*, vol. 8, pp. 88026-88041, 2020.
- [18] J. Zhao, H. Mu, Q. Zhang and H. Zhang, "ResNet-WGAN-Based End-to-End Learning for IoV Communication With Unknown Channels," *IEEE Internet of Things Journal*, vol. 10, no. 19, pp. 17184-17192, 1 Oct.1, 2023
- [19] C. Wang et al., "Pulmonary Image Classification Based on Inception-v3 Transfer Learning Model," *IEEE Access*, vol. 7, pp. 146533-146541, 2019.
- [20] B. Chen, X. Liu, Y. Zheng, G. Zhao and Y. -Q. Shi, "A Robust GAN-Generated Face Detection Method Based on Dual-Color Spaces and an Improved Xception," *IEEE Transactions on Circuits and Systems for Video Technology*, vol. 32, no. 6, pp. 3527-3538, June 2022.
- [21] G. Wang et al., "1D-CNN Network Based Real-Time Aerosol Particle Classification With Single-Particle Mass Spectrometry," *IEEE Sensors Letters*, vol. 7, no. 11, pp. 1-4, Nov. 2023, Art no. 6007904.
- [22] J. Liu, L. Ma and Z. He, "Underwater Visible Light Mobile Communication Using a Gain Feedback Control Method With Dynamic Threshold," *IEEE Photonics Journal*, vol. 15, no. 6, pp. 1-6, Dec. 2023, Art no. 7305306.
- [23] A. Vats, M. Aggarwal and S. Ahuja, "Outage analysis of AF relayed hybrid VLC-RF communication system for E-health applications," 2017 International Conference on Computing, Communication and Automation (ICCCA), Greater Noida, India, 2017, pp. 1401-1405.
- [24] Mansour, I. M. (2022). Effective Visible Light Communication System for Underground Mining Industry. *Indonesian Journal of Electrical Engineering and Informatics (IJEI)*, 8(2). <https://doi.org/10.52549/ijeei.v8i2.1978>
- [25] Zhang, Y., Wang, Y., & Li, H. (2023). A Visible Light 3D Positioning System for Underground Mines Based on Convolutional Neural Network Combining Inception Module and Attention Mechanism. *Photonics*, 10(8), 918. <https://doi.org/10.3390/photonics10080918>